BL-11D/ 2017G638

Calibration of a CCD-Based Energy Monitor for High Power Soft X-Ray Lasers

Thanh-Hung DINH[1,*], Masaharu NISHIKINO[1], Masahiko ISHINO[1],
Takeshi HIGASHIGUCHI[2], and Tadashi HATANO[3]
[1] Kansai Photon Science Institute, National Institutes for Quantum and Radiological Science and Technology (QST), 8-1-7 Umemidai, Kizugawa, Kyoto 619-0215, Japan,
[2] Department of Electrical and Electronic Engineering, Faculty of Engineering and Center for Optical Research and Education (CORE), Utsunomiya University, 7-1-2 Yoto, Utsunomiya, Tochigi 321-8585, Japan
[3]Institute of Multidisciplinary Research for Advanced Materials (IMRAM), Tohoku University, 2-1-1 Katahira, Aoba-ku, Sendai 980-8577, Japan

1 Introduction

The interaction of a solid material with focused, intense pulses of x-ray radiations creates a strong electronic excitation state within an ultra-short time and on ultra-small spatial scales. This offers the possibility to control the response of a material on a spatial scale of less than a nanometer which is crucial for the next generation of nano-devices [1]. So far, generation of a short duration pulse of coherent x-ray radiation has been realized by techniques as well-known as laser-driven coherent x-ray sources, and free electron laser (FEL). Plasma-based x-ray laser (XRL), beside high harmonic generations (HHGs), is one of laser-driven coherent x-ray sources having along been studied. The population inversion of XRL is usually created by the electron collisional excitation in hot and dense plasma medium produced by intense optical laser pulses. The advantages of XRLs are their compactness – table-top scales, and the narrow spectral line of the emitted radiation. In National Institutes for Quantum and Radiological Science and Technology (QST), we have a Ni-like Ag plasma XRL operated at a wavelength of 13.9 nm with a narrow bandwidth of $\Delta\lambda/\lambda \leq 1 \times 10^{-4}$, a pulse duration of 7 ps and a pulse energy of sub-μJ [2]. The XRL has been used to investigate damage thresholds of solid materials. Recently, x-ray free-electron lasers (XFELs) – the fourth generation light sources have been introduced in the large-scale facilities of modern synchrotrons. In Japan, the beamline-1 (BL1) at the Japanese x-ray free-electron laser facility, SACLA, has started operation for users, providing FEL radiations at soft x-ray regions (around 13 nm) with a pulse duration of ~70 fs and a pulse energy of up to 100 μJ [3]. A critical issue of both XRLs and XFELs is their SASE (self-amplified spontaneous emission) lasing mode which usually leads to a large shot-by-shot fluctuation of the laser output. Therefore, a monitor that indicates energy of each laser pulse, is essential for quantitative analysis.

For the illumination experiments using the 13.9-nm XRL at QST and the soft x-ray free-electron laser (SXFEL) at SACLA, an energy monitor which consists of an x-ray charge-coupled device (CCD) image sensor and x-ray filters has been employed. Here we report the calibration of the CCD-based energy monitor and its preliminary performance in application study.

2 Configuration of the CCD-based energy monitor

The schematic view of the CCD-based energy monitor is depicted in Fig. 1. A set of thin-film zirconium (Zr) and silicon (Si) filters is motorized and be used as an attenuator to regulate the pulse energy. So far, there are many advanced energy detectors which can operate at very high repetition rate (up to 100 kHz), e.g., commercial x-ray photo-diodes, gas monitor detector [4]. Although, an x-ray CCD image sensor can only be operated at a relatively low repetition rate ranging from 1 Hz to few-tens Hz, its advantage is both laser pulse energy and its spatial beam profile can be monitored simultaneously. From the beam profile data, one can retrieve the illuminated laser spot on the target surface by a ray tracing calculation. The sensitivity of x-ray CCD camera and the transmittance of x-ray filters were calibrated by using synchrotron radiation from the BL-11D beamline of the PF.

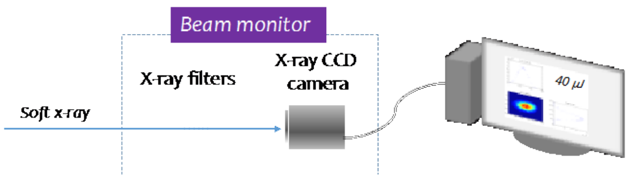

Fig. 1: Schematic view of the CCD-based energy monitor

3 Measurement of the sensitivity of x-ray CCD cameras

The detailed procedure of the calibration has been reported previously in Ref. 5. In briefly, the experimental setup is shown in Fig. 2(a). To minimize the influence of the impure light included in the beamline, an aluminum (Al) filter with a thickness of 200 nm was used. A calibrated AXUV100G x-ray diode was used to determine the number of photons incident onto the x-ray CCD camera. The CCD chip was cooled at −50 °C with a pressure in the calibration chamber of 5×10^{-5} Pa. Since the high vacuum degree was achieved, influence of the residual contamination such as nitrogen, water vapor, and carbon compounds, which deposit and condense onto the cooled CCD surface, was negligibly small. This type of contamination usually can be removed by warming up the chip.

Figure 2(b) indicates an image recorded by the CCD camera setting at an exposure time of 0.5 sec and a pixel readout rate of 3 MHz. The beamline shutter was opened until the readout finished. The red- and yellow colored circles in Fig. 2(b) indicated the smearing parts caused by the opening process of the digital shutter and the readout process of the CCD camera, respectively. As shown in Fig. 3, the count number of CCD camera linearly increases with raising the exposure times. The count number of the smearing is equal to the count number at the exposure time of 0 second; therefore one can derived it from the fitting equation of the data as show in Fig. 2(c) . By considering amount of the smearing, the effective exposure time was calculated to be 1.54 sec with a discrepancy of less than 3%.

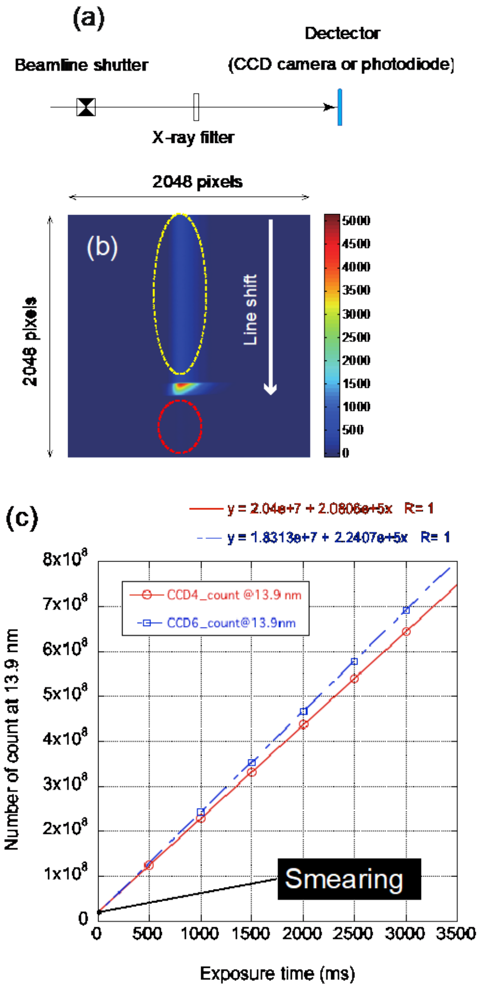

Fig. 2: Calibration of an x-ray CCD camera. (a) is experimental setup. (b) is a typical image recorded by the CCD camera. (c) indicates the count number of the CCD cameras as function of the exposure time for the wavelength of 13.9 nm.

Figure 3 indicates the measured sensitivity of the CCD cameras at the soft x-ray region. Each CCD camera usually has a different sensitivity curve. An obvious reason is that the sensitivity depends on performance of the assembled components. The CCD chip would also be degraded upon exposure of intense x-ray radiation. Therefore, a regularly calibration is strongly recommended for CCD cameras used in x-ray region.

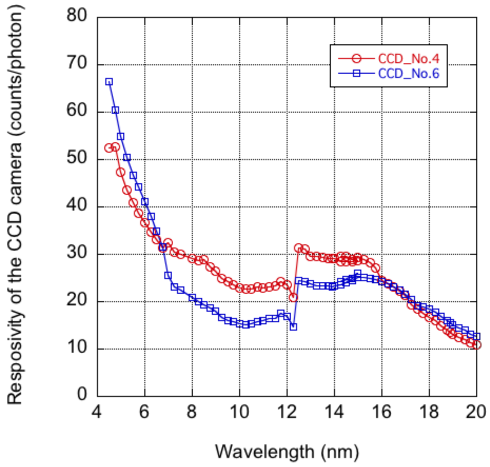

Fig. 3: The sensitivity curves of x-ray CCD cameras.

4 <u>Characterization of a zirconium filter</u>

We have also measured the transmittance of a Zr filter with a nominal thickness of 200 nm by the x-ray photodiode. The measured result, denoted by the red-circles in Fig. 4, is well-fitted with the solid- blue curve calculated from the data base [6] with the thickness of Zr layer of 184 nm and ZrO_2 layer of 56 nm. This result implies that the surface of the Zr filter had been oxidized. Our detailed investigation shows that the oxidation of Zr filters would start during their production process. The maximum thickness of ZrO_2 layer was observed to be of ~70 nm for Zr filters which have been used in for more than three years. It should be noted that our x-ray filters have been safekeeping in a desiccator after usage.

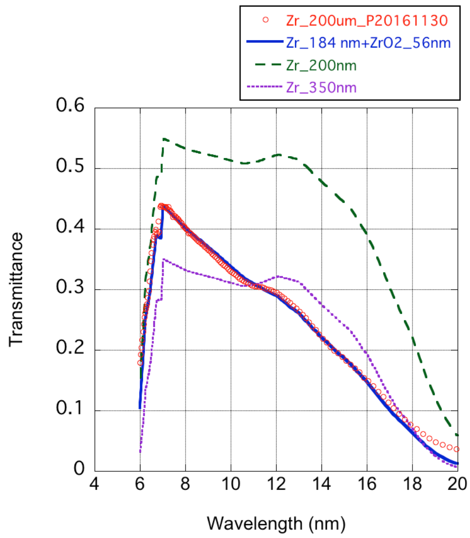

Fig. 4: Transmittance of a Zr filter with a nominal thickness of 200 nm. The red circles is the measured value. The green-dashed-line and purple dotted-line are the transmittance of Zr filters calculated from the data base for the thickness of 200 nm and 350 nm, respectively. The solid-blue-line is the calculated curve with the thicknesses of Zr and ZrO_2 layers of 184 nm and 56 nm, respectively.

5 Operation of the energy monitor in application studies

The calibrated CCD-based energy monitor has been installed into the XRL and the SACLA SXFEL beam lines for the damage studies of several solid materials [1,7]. Figure 5(a) depicts the schematic diagram of the irradiation experiment performed at the SACLA SXFEL. Single x-ray pulse from the SXFEL is focused onto the surface of solid materials by using a Kirkpatrick-Baez (K-B) mirrors. The target surface is normal with respect to the incident laser beam. The diameters of the laser spot size at full width at half maximum, which were measured by knife-edge scanning, were ~5.5 μm and ~4.5 μm for horizontally and vertically, respectively. An attenuator consist of calibrated thin-film filters was motorized to regulate the pulse energy. These filters were also helpful to block the undesired high harmonic orders of the FEL radiation. During the experiment, the pulse energy was monitored by a gas detector monitor on a shot-to-shot basis with a relative uncertainty of 10%. The throughput energy was evaluated by the calibrated CCD monitor. Figure 5(b) indicates the linearity of the CCD-based energy monitor versus the gas detector monitor.

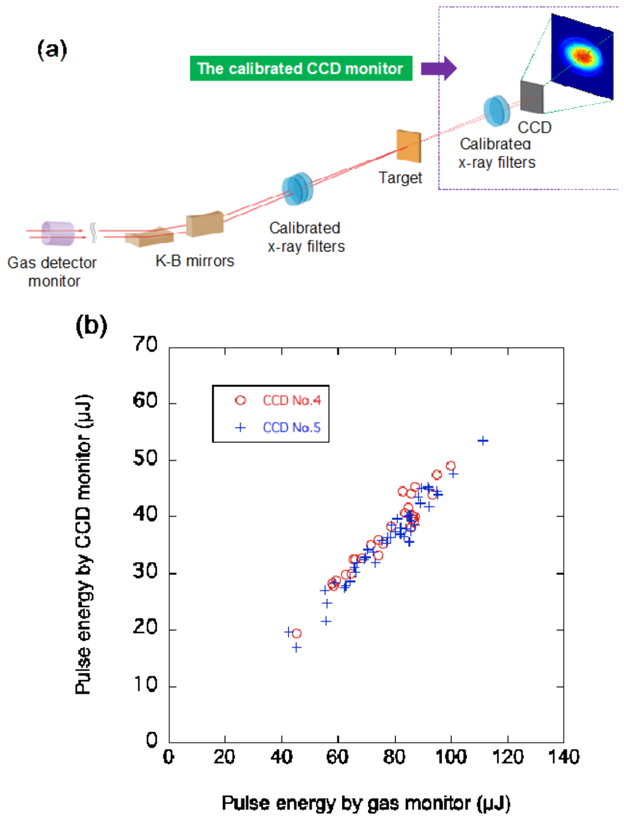

Fig. 5: Operation of the CCD-based energy monitor in an application study at the SACLA SXFEL. (a) Schematic view of the damage test experiment. (b) indicates the linearity of the CCD-based energy monitor versus the gas detector monitor which has been installed at the SACLA SXFEL.

In summary, the calibration of each optical element is very importance for quantitative studies, which use the radiation in soft x-ray region. Here the calibration of the CCD-based energy monitor using synchrotron radiations from the soft x-ray beam line BL-11D of the PF has been reported. Such energy monitor is essential instrument for the quantitative experiment of light-matter-interaction using the XRL and the SXEFL.

Acknowledgement

A part of this study was supported by support from JSPS KAKENHI Grant Number JP19K15402.

References

1. Dinh, T.-H. *et al.* Controlled strong excitation of silicon as a step towards processing materials at sub-nanometer precision. *Commun. Phys.* **2**, 150 (1–9) (2019).
2. Nishikino, M. *et al.* Demonstration of a soft-x-ray laser at 13.9 nm with full spatial coherence. *Phys. Rev. A* **68**, 061802 (2003).
3. Owada, S. *et al.* A soft X-ray free-electron laser beamline at SACLA: The light source, photon beamline and experimental station. *J. Synchrotron Radiat.* **25**, 282–288 (2018).
4. Tiedtke, K. *et al.* Gas detectors for x-ray lasers. *J. Appl. Phys.* **103**, 094511 (2008).
5. Dinh, T.-H. *et al.* Evaluation of a flat-field grazing incidence spectrometer for highly charged ion plasma emission in soft x-ray spectral region from 1 to 10 nm. *Rev. Sci. Instrum.* **87**, 123106 (2016).
6. Powell, C. J. & Jablonski, A. Evaluation of Calculated and Measured Electron Inelastic Mean Free Paths Near Solid Surfaces. *J. Phys. Chem. Ref. Data* **28**, 19 (1999).
7. Mikami, K. *et al.* Laser-induced damage thresholds and mechanism of silica glass induced by ultra-short soft x-ray laser pulse irradiation. *Opt. Lett.* **45**, 2435 (2020).

* dinh.thanhhung@qst.go.jp